Journal of
Materials Chemistry C

PAPER

View Article Online
View Journal | View Issue

Check for updates

Cite this: *J. Mater. Chem. C*, 2019, 7, 14232

Received 23rd July 2019,
Accepted 17th October 2019

DOI: 10.1039/c9tc04004h

rsc.li/materials-c

Both increasing the Iso-to-Col transition and lowering the solidifying temperatures of a triazine-based dendrimer by introducing CN polar groups in the dendritic core†

Cheng-Hua Lee,[a] Chun-Chi Huang,[b] Chia-Ying Li,[a] Long-Li Lai, *[a] Jey-Jau Lee[c] and Hsiu-Fu Hsu*[b]

Two new triazine-based dendrimers **1a** and **1b**, containing $-NY(CH_2)_3NY-$ linkers between two G_3 dendrons (**1a**: Y = Bz, **1b**: Y = 4-cyanoBz; Bz = benzyl), were successfully prepared in ∼32 and ∼34% yields, respectively. Compared with dendrimer **1c** that contains $-NH(CH_2)_3NH-$ linkers between two G_3 dendrons, dendrimer **1a** exhibits a similar mesogenic range to **1c**, but **1b** possesses a broader mesophase-temperature range than **1c**. Surprisingly, dendrimer **1b** not only increases the isotropic-phase-to-columnar-mesophase (Iso-to-Col) transition temperature but also lowers the solidifying temperature on cooling. It is believed that the CN groups in the dendritic linker of **1b** increase both the molecular interaction between dendrimers, leading to its increasing Iso-to-Col transition temperature, and dendritic distances within columns, leading to its decreasing solidifying temperature.

Introduction

Different from polymers, dendrimers with core, linker and peripheral moieties, are tree-like molecules with a well-defined chemical structure and a single molecular weight.[1] Their physical properties are thus interesting and probably predictable.[1e–j] Particularly, multiple functions can be specifically tailored onto one molecule for potential applications in various fields,[2–7] and therefore great attention has been focused on dendrimers recently. Although columnar liquid crystalline (LC) dendrimers, exhibiting uniform packing and non-grained boundaries, have been found suitable for applications in electronic and optoelectronic devices,[8,9] controlling their conformations to exhibit mesogenic behaviors is rather difficult, because their conformations are versatile due to the various combinations of the constructing units and peripherals. However, liquid crystallinity may be attained by installing mesogenic units in dendritic moieties.[10–13]

Triazine-based dendrimers, studied by Takagi and Simanek, respectively,[14] have been shown to possess significant face-to-face interactions between triazine moieties,[15] and result in columnar mesophase formation.[16] We have recently revealed that columnar liquid crystalline dendrimers may be expected by bridging two triazine-based dendrons by semi-rigid linkers for limited conformational freedom.[16e,f] The angle of the two dendrons, influenced by an odd or even number of the alkyl unit in the $-NY(CH_2)_nNY-$ (Y = H) bridge, was found to be crucial for inducing liquid crystallinity.[16e] Steric hindrance of the bridge can also induce liquid crystallinity by tuning the packing of the two dendrons.[16f] However, the mesogenic ranges of the dendrimers, induced by two previous approaches, were rather narrow, all less than 34-degrees.[16e,f] Combining both strategies, we hope to prepare dendrimers with a broad mesophase-temperature range, which is valuable for potential application. Dendrimers **1a** and **1b**, containing the $-NY(CH_2)_3NY-$ linker between two G_3 moieties (**1a:** Y = Bz, **1b:** Y = 4-cyanoBz; Bz = benzyl), were therefore prepared. Compared with **1c**, containing the $-NH(CH_2)_3NH-$ linker, the mesogenic range of **1a** is not expanded on cooling, but the mesogenic range of **1b** is broader than those of **1a** and **1c** (Fig. 1). The CN groups in the dendritic linker not only increase the isotropic-phase-to-columnar-mesophase (Iso-to-Col) transition temperature but also lower the solidifying temperature on cooling, thus significantly broadening the mesogenic ranges.

Discotic columnar (DC) liquid crystals have potential applications in opto-electronic devices due to their long-range self-assembling properties.[17a] Particularly, colorless and soluble DC liquid crystals are good candidates for solvating specific materials such as carbon nanotubes.[17b] It has been proved that triazine-based

---

[a] *Department of Applied Chemistry, National Chi Nan University, No. 1 University Rd., Puli, Nantou 545, Taiwan. E-mail: lilai@ncnu.edu.tw*

[b] *Department of Chemistry, Tamkang University, No. 151, Yingzhuan Rd, New Taipei City 251, Taiwan. E-mail: hhsu@mail.tku.edu.tw*

[c] *National Synchrotron Radiation Research Center, No. 101 Hsin-Ann Rd., Hsinchu 300, Taiwan*

† Electronic supplementary information (ESI) available. See DOI: 10.1039/c9tc04004h

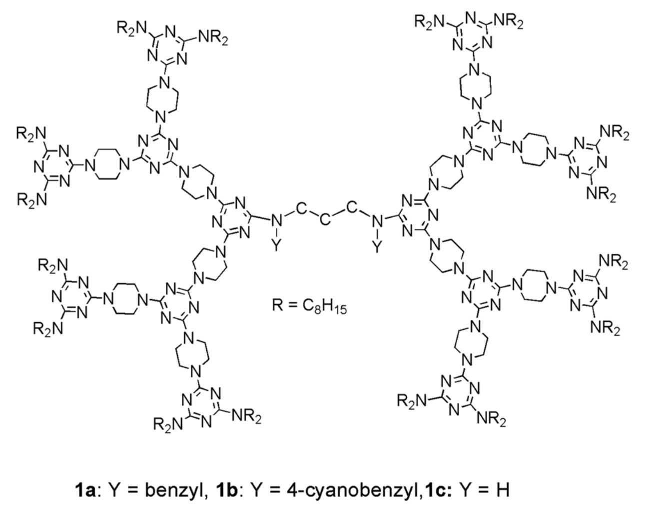

Fig. 1 The molecular structures of dendrimers **1a–1c**.

dendrimers exhibit good solubility in organic solvents and columnar phases on thermal treatment.[16] However, their solidifying temperatures are rather high. By introducing a polar CN group into the linker of triazine-based dendrimers, we have successfully broadened the mesogenic range and lowered the solidifying temperature on cooling, which may increase their value in application.

Experimental section

Sample characterization by POM

In the first thermal process, dendrimer **1a** was rapidly heated to its isotropic temperature, and then cooled to 30 °C at a rate of 20 °C min^{-1}. **1a** was then heated at 5 °C min^{-1} rate and cooled at 0.5 °C min^{-1} rate in the second thermal cycle. The treatment for dendrimer **1b** was similar.

Sample characterization by DSC

Dendrimer **1a** was heated to 170 °C and then allowed to cool to room temperature at a rate of 10 °C min^{-1} in the first thermal cycle. The heating and cooling rates were maintained at a rate of 5 °C min^{-1} in the second thermal cycle. The transition temperature and the corresponding enthalpies were recorded in the second thermal cycle. A similar process was applied to dendrimer **1b** accordingly.

The procedure for preparing dendrimer 1a

G3-Cl (0.9 g, 0.3 mmol) and *N*,*N*-dibenzylamino-propane (0.08 g, 0.3 mmol) were added to dry THF (25 mL). The solution was heated at 70 °C for 24 hour. **G3-Cl** (0.9 g, 0.3 mmol) and potassium carbonate (0.21 g, 1.5 mmol) were then added. The mixture was then heated at 170 °C for 72 hour in a sealed tube for another 24 hour. The solvent was removed at reduced pressure and water (50 mL) was then added. The resulting solution was extracted with CH_2Cl_2 (30 mL × 2). The combined extracts were washed with water (25 mL), dried over $MgSO_4$, and then evaporated at reduced pressure, and the residue was purified by chromatography to give a crude solid, which was further recrystallized by using CH_2Cl_2–CH_3OH (20 : 1) to give dendrimer **1a** in 34.2% yield (0.64 g). ^1H NMR (300 MHz, $CDCl_3$, 25 °C, TMS): δ 0.88 (s br., 96H, 32 × CH_3), 1.28 (s br., 320H, 160 × CH_2), 1.56 (s br., 64H, 32 × CH_2), 3.46 (s, 68H, 34 × CH_2), 3.80 (s, 100H, 50 × CH_2), and 7.23 (s br., 10H, Ar-H). ^{13}C NMR (75 MHz, $CDCl_3$, 25 °C, TMS): δ 14.3, 22.8, 27.3, 28.3, 29.5, 29.6, 29.8, 32.6, 43.3, 47.4, 165.2, and 165.6. MS cacld for $C_{363}H_{660}N_{84}$ $[M + K]^+$: 6239.8; found 6239.9. Elemental analysis calcd for $C_{363}H_{660}N_{84}$: C 70.30; H 10.73; and N 18.97; found C 69.88; H 10.84; and N 18.89.

Dendrimer **1b** was obtained in a similar manner (0.61 g, 32.6%). ^1H NMR (300 MHz, $CDCl_3$, 25 °C, TMS): δ 0.86 (s br., 96H, 32 × CH_3), 1.27 (s br., 320H, 160 × CH_2), 1.58 (s br., 66H, 33 × CH_2), 3.45 (s, 68H, 34 × CH_2), 3.79 (s br., 96H, 48 × CH_2), 4.78 (s, 4H, 2 × CH_2), 7.29 (d, *J* = 7.8Hz, 4H, Ar-H), and 7.53 (d, *J* = 7.8Hz, 4H, Ar-H). ^{13}C NMR (75 MHz, $CDCl_3$, 25 °C, TMS): δ 14.3, 22.8, 27.3, 27.5, 28.3, 29.6, 29.8, 30.5, 32.1, 43.3, 47.1, 47.4, 165.3, and 165.6. MS cacld for $C_{365}H_{658}N_{86}$ $[M]^+$: 6251.7; found 6251.8. Elemental analysis calcd for $C_{365}H_{658}N_{86}$: C 70.13; H 10.61; and N 19.27; found C 69.82; H 10.62; and N 19.12.

Results and discussion

Dendron **G_3-Cl** was synthesized by our previously reported method.[16] Dendrimer **1a** was prepared from the reaction of **G_3-Cl** with *N*,*N*-dibenzylaminopropane[18] in ∼34% yield after purification (Scheme 1). Dendrimer **1b** was obtained in ∼33% yield in a similar manner. Dendrimers **1a** and **1b** were studied by ^1H and ^{13}C NMR spectroscopy, and then characterized by elemental analysis as well as MALDI-TOF mass spectrometry. The mass spectrum of **1a**, represented as an example, is shown in Fig. 2; a peak of *m*/*z* at 6240.0 from the $[M + K]^+$ ion is clearly observed in the spectrum for characterization.

Similar to **1c**,[16e] dendrimers **1a** and **1b** were investigated by polarizing optical microscopy (POM), showing a columnar mesophase (Fig. 3). Detailed thermal behaviors of these dendrimers, studied by differential scanning calorimetry (DSC) (Fig. S4, ESI†), are summarized in Scheme 2. Dendrimer **1a** enters the columnar mesophase at ∼114.9 °C and solidifies at ∼82.2 °C on cooling.

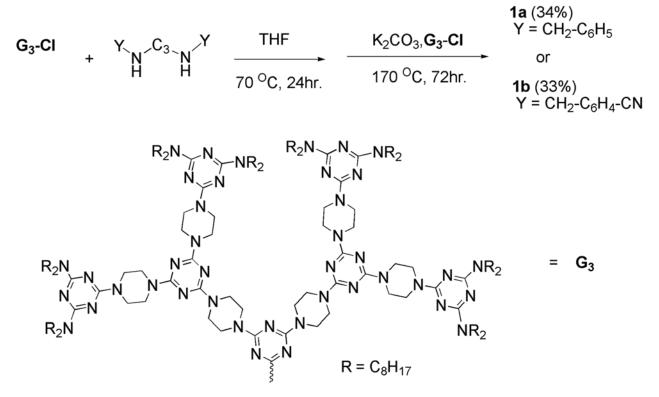

Scheme 1 Preparation of dendrimers **1a** and **1b**.

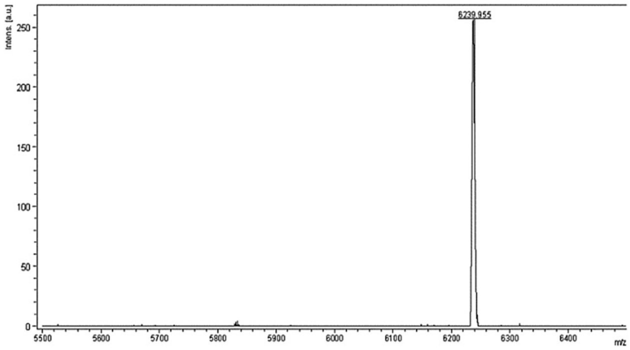

Fig. 2 The MALDI-TOF mass spectrum of **1a**.

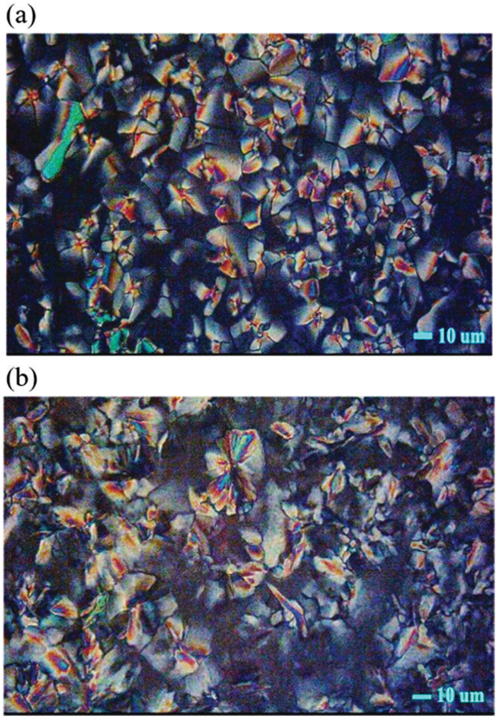

Fig. 3 The POM textures of **1a** (a) and **1b** (b), which were taken at 110 °C and 130 °C, respectively, on cooling at a rate of 0.5 °C min^{-1} in the second thermal process.

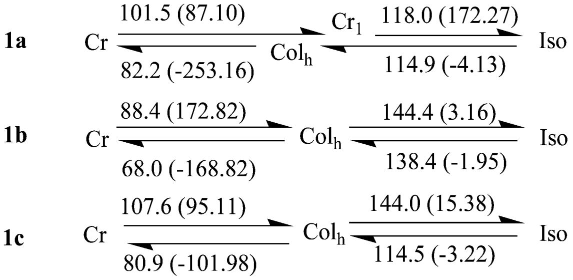

Scheme 2 The corresponding enthalpies (kJ mol^{-1}), in parentheses, at phase transition temperatures of dendrimers **1a**, **1b** and **1c**. Cr and Cr$_1$, Col$_h$ and Iso represent the crystalline, hexagonal columnar and isotropic phases, respectively.

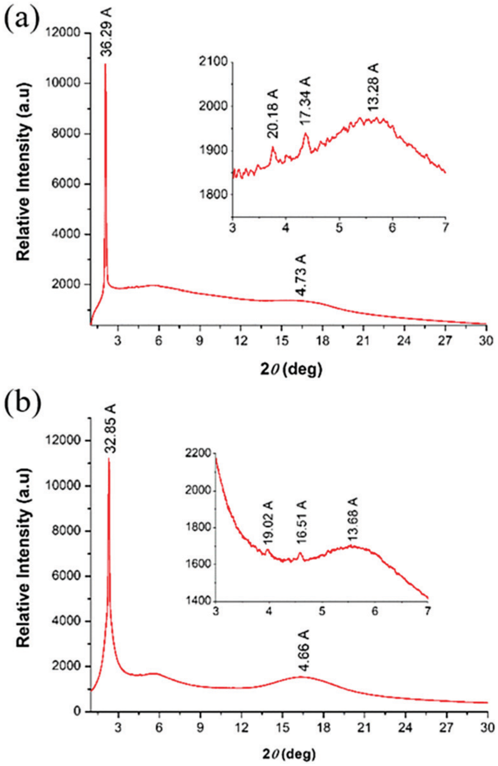

Fig. 4 (a) The powder-XRD patterns **1a** (a) and **1b** (b), which were taken at 110 °C and 130 °C, respectively, on cooling at a rate of 1 °C min^{-1}.

However, dendrimer **1c** becomes mesogenic at ~114.5 °C and then solidifies at ~80.9 °C. The mesophase-temperature range of **1a** is ~33-degrees on cooling, which is similar to that of **1c** (Scheme 2). Dendrimer **1b** enters the mesophase at ~138.4 °C prior to solidifying at ~68.0 °C on cooling to lead to a ~70-degree mesogenic range, wider than those of **1a** and **1c**.

The columnar phases of **1a** and **1b** were further studied by powder X-ray diffraction (XRD). As shown in Fig. 4a, a sharp peak at 36.29 Å, in the small-angle region of powder XRD of **1a**, arises from the d_{10} reflection. Two additional weak signals at 20.18 and 17.34 Å in the corresponding regions result from d_{11} and d_{20} reflections, respectively. The signal at 13.28 Å can be assigned to d_{21}; however, the line-shape (broadness or line-width) of this signal is very different from that of d_{10} to exclude the possibility. The signal assignment to the intra-columnar disc correlation shall be verified by XRD of the aligned samples. However, attempts to obtain the aligned samples are not successful. The broadness of the signal at 13.28 Å is a characteristic of a weak correlation and is therefore assigned to the thickness of a fluffy disc, *i.e.* intracolumnar correlation. Similar to **1c**, compounds **1a** and **1b** do not show π–π correlations, typically at *ca.* 3.5 Å. The signal due to π–π interactions may be too weak to be revealed by XRD or to be hidden in the wide-angle halo at 4.73 Å, typically from the liquid-like correlations of alkyl chains. The XRD reflection pattern indicates that **1a** possesses a hexagonal columnar phase with the calculated lattice constant *a* of 41.9 Å. Dendrimer **1b** has a similar XRD pattern to **1a**, indicating that their mesophases are the same. The corresponding lattice constant *a* of **1b** was calculated to be 38.4 Å.

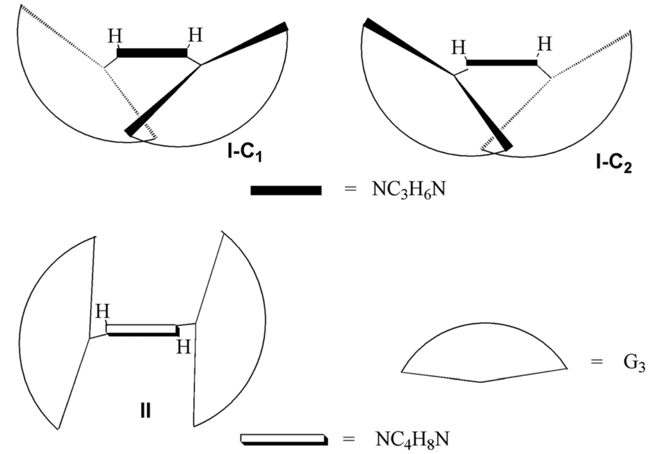

Fig. 5 The possible conformations of the dendrimers with –YN(CH$_2$)$_4$NY– and –YN(CH$_2$)$_3$NY– (Y = H) bridges.

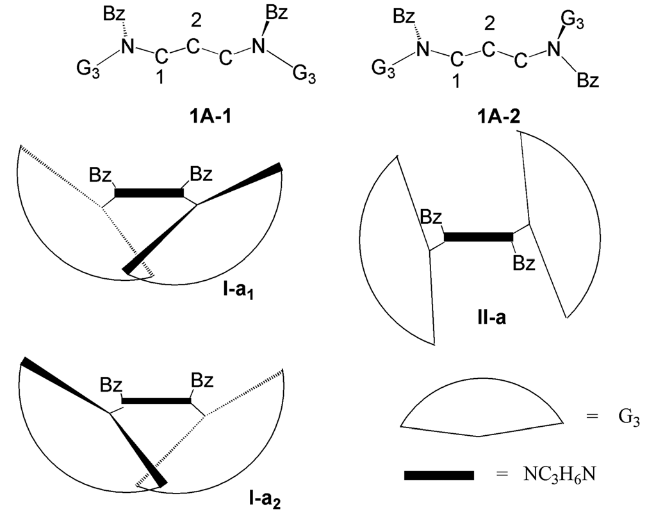

Fig. 6 The possible conformations of dendrimer **1a**.

As indicated previously,[16e] the morphology of dendrimers with –NY(CH$_2$)$_n$NY– (Y = H; n = 2 and 4) linkers is different from that with –NY(CH$_2$)$_n$NY– (Y = H; n = 3 and 5) linkers. The dendrimers with the even-carbon linker prefer the arrangement of the two G$_3$ moieties in the *anti*-position for decreasing the repulsion between the linker and G$_3$. The dendrimers with the odd-carbon linker favor the two G$_3$ moieties in the *syn*-position, thus leading to overlap of the two dendrons. For example, two skeletons of the dendrimers (Y = H; n = 4 and 3) are shown in Fig. 5. When two G$_3$ moieties are overlapped in the *syn*-position, one G$_3$ moiety may be under or above the other G$_3$. Therefore, dendrimer **1c** possesses two isomers, *i.e.* **I-C$_1$** or **I-C$_2$**, and was observed to exhibit LC phases on thermal treatment due to the isomeric effect. However, the dendrimer with the –NY(CH$_2$)$_4$NY– linker (Y = H) does not show any LC phase because this dendrimer has only one isomer, *i.e.* **II**, in the condensed-phase stacking.[16e]

In the continuing study, dendrimer **1a** with the –NY(CH$_2$)$_3$NY– linker (Y = Bz) was prepared to examine the mesogenic properties from the steric and odd–even effect of the linker. When two N–H moieties were replaced by two *N*-benzyl groups, the repulsion between H (at C2) atoms and benzyls (Bz) increases; this will result in dendrimer **1a** having two skeletons, *i.e.* **1A-1** and **1A-2** (Fig. 6).[16e,f] Because the repulsion between the linker and Bz in the **1A-1** skeleton is less than that between the linker and G$_3$ in the **1A-2** skeleton, more **1a** molecules have the **1A-1** skeleton with two G$_3$ moieties in the *syn*-position and less **1a** molecules possess the **1A-2** skeleton with two G$_3$ moieties in the *anti*-position, as previously discussed.[16f] Therefore, **1a** possesses three isomers, *i.e.* **I-a1**, **I-a2** and **II-a** in the condensed-phase stacking but **1c** has only two isomers *i.e.* **I-C$_1$** and **I-C$_2$**. As expected, the first phase-transition (~101.5 °C) and the clearing (~118.0 °C) temperatures of **1a** on heating are thus lower than those of **1c** (~107.6 and ~144.0 °C), respectively.[16e,f] Although the steric effect in the –YN(CH$_2$)$_4$NY– linker between G$_3$ moieties successfully converted the non-LC dendrimer to the LC dendrimer,[16f] this approach in the –YN(CH$_2$)$_3$NY– bridge does not effectively expand the mesogenic range; the mesogenic range of **1a**, ~33-degrees on cooling, is similar to that of **1c** (Scheme 2). Dendrimer **1b** with the –NY(CH$_2$)$_3$NY– linker (Y = 4-cyanoBz) was thus further prepared to affect the stacking morphology, aiming to improve the mesogenic properties. Surprisingly, the Iso-to-Col transition temperature (~138.4 °C) of **1b** on cooling is higher than that of **1c**, and the solidifying temperature (~68.0 °C) of **1b** is lower than that of **1c**, resulting in significant expansion of the mesophase-temperature range of **1b** when compared with those of **1a** and **1c**.

To have an understanding of the CN effect upon expanding the mesogenic range of the dendrimers, an attempt to optimize the conformation of the dendrimers **1a** and **1b** was undertaken. Because most **1a** molecules have the **1A-1** skeleton, as previously discussed, it was thus used as a model for simulation. For simplicity, the disk framework of **1a** (without peripheral amino moieties) was simulated by the MM3 method in the Cache program in the air phase. Based on our previous method,[16e,f] the disk framework of **1a** was optimized first, and two benzyl groups were incorporated onto the optimized **1a** framework. After optimization, two morphologies of framework **1a** were obtained; one had two benzyl groups in the *cis*-position and the other had two benzyl groups in the *trans*-position when viewed along the disc plane (Fig. 7).

The energy for the *cis*-morphology, 53.06 kcal mol^{-1}, is quite similar to that for the *trans*-morphology, 54.30 kcal mol^{-1}. Similarly, two molecular morphologies of **1b** were accordingly obtained and the energies for the *cis*- and *trans*-morphologies are 53.67 and 54.89 kcal mol^{-1}, respectively. The energy differences between *cis*- and *trans*-morphologies for both dendrimers are not significant, and therefore both morphologies may appear in their condensed-phase stackings. Interestingly, the morphology of **1a** for each molecule in the air phase, either in *cis* or *trans* conformation, is very similar to that of **1b**, respectively; therefore, both dendrimers **1a** and **1b** not only exhibit a similar stacking in the condensed-phase, confirmed by the powder-XRD study, but also have the columnar hexagonal arrangement as in **1c**. Additionally, both Bz and 4-cynaoBz moieties are definitely not parallel to the disc frame of the dendrimers. The congestion between benzyl or cyanobenzyl groups, to some extent, leads to the columnar slice of **1a** (13.28 Å)

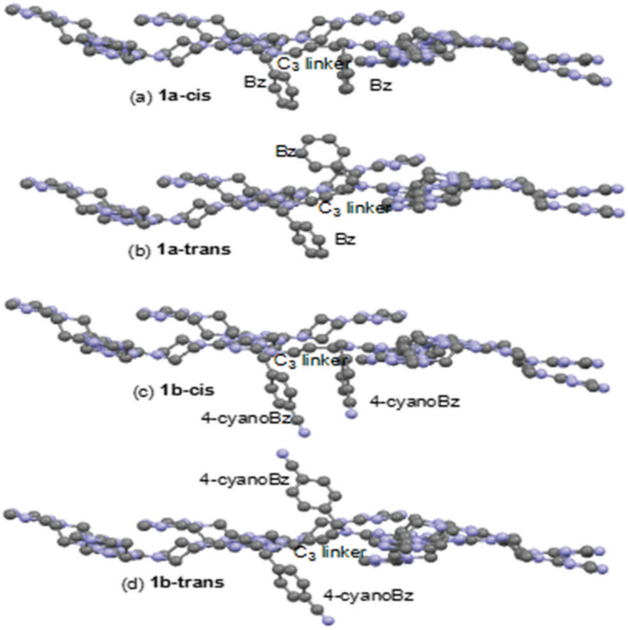

Fig. 7 The possible conformations (side views) of dendrimers **1a**, (a) *cis*- and (b) *trans*-isomers, and **1b**, (c) *cis*- and (d) *trans*-isomers. N and C atoms are demonstrated by purple and gray colours, respectively, and Hs are omitted.

becoming slightly larger than that of **1c** (13.14 Å) at the same temperature of 110 °C. Columnar slices of **1c** at 94, 105, 110, and 114 °C remain similar, *i.e.* temperature independent (Fig. S8/Table S1, ESI†). The columnar slice of **1b**, 13.68 Å, at 130 °C is larger than those of **1a** and **1c** at 110 °C. If the temperature independence of the columnar slice of **1c** also applies to **1b** with a similar dendrimer chemical framework, the larger columnar slice of **1b** than those of **1a** and **1c** can be realized by the strong repulsion of CN polarity. Although the CN polarity may also result in intermolecular dipole–dipole interaction, this mutual attraction should be less significant due to the CN···NC arrangement between the dendrimers; as shown in Fig. 7, because of the limited space between the two G_3 dendrons, the influence of the CN moiety more effects in the axial direction. Interestingly, at the same temperature of 110 °C, the d_{10}, 36.29 Å, of **1a** is considerably larger than that of **1c**, 32.98 Å. The d_{10} values of **1c** upon cooling at 104, 110, 105, and 94 °C increase but to a small extent between 32.86 and 32.98 Å. The d_{10} value (32.85 Å) of **1b** at 130 °C is only slightly less than that of **1c** at 110 °C. Considering the temperature dependence of d_{10} of **1c**, the difference in d_{10} between **1c** and **1b** is negligible. Because dendrimers **1a–1c** all have the same dendrons and similar powder-XRD patterns, it is reasonably assumed that **1a–1c** possess the same number of molecules in each column slice. Under such an assumption, the steric hindrance effect from the benzyl group in **1a** significantly leads to mutual gliding of molecules within columns but slightly increase the disc-to-disc distance between molecules in comparison with **1c**. The strong polarity of the 4-CN benzyl group in **1b** obviously enlarges the corresponding disc-to-disc distance for balancing the polar repulsion between molecules within columns and therefore its gliding effect is not significant.

Table 1 Calculated data of compounds **1a–1c**[a]

Cpd	Phase	M_r	T (°C)	V_m (Å^3)	V_{cell} (Å^3)	V_m/V_{cell}
1a	Col$_h$	6202	110	10981.1	13686.3	0.80
1b	Col$_h$	6252	130	11225.9	11510.1	0.98
1c	Col$_h$	6022	110	10662.4	11230.3	0.95

[a] M_r is the molecular weight. V_m and V_{cell} are the molecular and cell volumes respectively.

For further confirming our study, the molecular volumes (V_m), cell volumes (V_{cell}), and V_m/V_{cell} of dendrimers **1a–1c** were calculated according to our previous report.[16e,f] The related results are demonstrated in Table S1 (ESI†). It should be noted that the XRD data of **1a** and **1c** were recorded at the same temperature of 110 °C and those of **1b** were recorded at 130 °C. Nevertheless, the temperature dependence of V_m/V_{cell}, from 0.95 at 114 °C to 0.93 upon cooling to 94 °C, was demonstrated from the variable-temperature XRD studies of **1c**. As similar numbers of molecules per cell for **1a–1c** are obtained, these dendrimers are supposed to have one molecule in a columnar slice. According to the literature,[19] the V_m/V_{cell} value of **1a**, **1b** and **1c** is calculated to be ∼0.80, ∼0.98 and ∼0.95, respectively (Table 1).

Definitely, at 110 °C, the V_m/V_{cell} of **1a** is smaller than that of **1c**, which indicates that the dendritic molecules of **1a** are more closely stacked than those of **1c**, as discussed in our previous report. Although the Bz group slightly increases the disc-to-disc distance between molecules, the Bz group also increasingly occupies the extra space between molecules. As a result, the first phase-transition and solidifying temperatures of both **1a** and **1c** on cooling are similar to each other, and their mesogenic ranges are thus comparable. The V_m/V_{cell} of **1b** at a higher temperature of 130 °C is greater than that of **1c**, indicating that the dendritic molecules of **1b** are less closely stacked than those of **1c** (Fig. 8), and thus a lower solidifying temperature was observed on cooling. However, the increased V_m/V_{cell} with the increasing temperature observed for **1c** may also apply to **1b** whose XRD was measured at a higher temperature. In addition, the CN groups may also increase the molecular interaction; this balances the less packing effect, and therefore the clearing

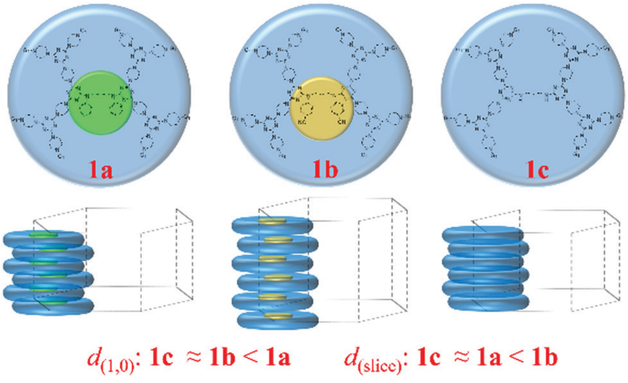

Fig. 8 The various arrangements of molecules **1a** (110 °C), **1b** (130 °C), and **1c** (110 °C) within hexagonal columns.

temperatures of **1b** and **1c** on heating are comparable. If dendrimers **1a** and **1b** are compared with each other, the polar effect can be more significantly observed; the clearing temperature of **1b** (~144.4 °C) is higher than that of **1a** (~118.0 °C) and the solidifying temperature of **1b** (~68.0 °C) is lower than that of **1a** (~82.3 °C). Thus, the strong CN polar group significantly broadens the mesogenic range of **1b** (~70-degrees). The reason that the CN moieties result in the increasing disc-to-disc distances is probably that the void space between G_3 moieties may not balance the polar repulsion and enlarging the dendritic disc-to-disc distance is thus necessary. The corresponding effect in small disc molecules to broaden the mesogenic phases has been investigated by Williams[20] and is in agreement with our study result.

Conclusions

In summary, dendrimers **1a** and **1b** were successfully prepared and observed to exhibit columnar mesophases on thermal treatment. Compared with **1c**, **1a** has a lower clearing temperature on heating due to the isomeric effect but a comparable mesogenic range on cooling because of its closer stacking. Dendrimer **1b** enters the columnar mesophase at a significantly lower temperature and becomes isotropic at a similar temperature on heating to **1c** due to the CN polarity. The Iso-to-Col_h transition temperature of **1b** is considerably higher than those of **1a** and **1c** on cooling, and the subsequent solidifying temperature of **1b** is lower than those of **1a** and **1c**. Therefore, the polar CN groups in dendrimers, significantly reducing the stacking efficiency, lowering the solidifying temperature and expanding considerably the mesogenic range, are interesting and have not been reported so far. This should be applicable to other types of dendrimers with semi-rigid linkers for preparing dendrimers with valuable applications.

Conflicts of interest

There are no conflicts of interest to declare.

Acknowledgements

We thank the National Chi Nan University and the Ministry of Science and Technology, Taiwan for financial support (105-2119-M-260-006-MY3).

Notes and references

1 (*a*) S. M. Grayson and J. M. J. Fréchet, *Chem. Rev.*, 2001, **101**, 3819; (*b*) B. A. Laurent and S. M. Grayson, *J. Am. Chem. Soc.*, 2011, **133**, 13421; (*c*) H. Akiyama, K. Miyashita, Y. Hari, S. Obika and T. Imanishi, *Tetrahedron*, 2013, **69**, 681; (*d*) R. Sharma, N. Kottari, Y. M. Chabre, L. Abbassi, T. C. Shiao and R. Roy, *Chem. Commun.*, 2014, **50**, 13300; (*e*) T. Yasuda, T. Shimizu, F. Liu, G. Ungar and T. Kato, *J. Am. Chem. Soc.*, 2011, **133**, 13437; (*f*) Y. Sagara and T. Kato, *Angew. Chem., Int. Ed.*, 2011, **50**, 9128; (*g*) T. Kato, J. Uchida, T. Ichikawa and T. Sakamoto, *Angew. Chem., Int. Ed.*, 2018, **57**, 4355; (*h*) T. Kato, T. Yasuda, Y. Kamikawa and M. Yoshio, *Chem. Commun.*, 2009, 729; (*i*) B. Soberats, M. Yoshio, T. Ichikawa, X. Zeng, H. Ohno, G. Ungar and T. Kato, *J. Am. Chem. Soc.*, 2015, **137**, 13212; (*j*) Y. Sagara, S. Yamane, M. Mitani, C. Weder and T. Kato, *Adv. Mater.*, 2016, **28**, 1073.

2 (*a*) D. Astruc, E. Boisselier and C. Ornelas, *Chem. Rev.*, 2010, **110**, 1857; (*b*) A. M. Caminade, A. Ouali, M. Keller and J. P. Majoral, *Chem. Soc. Rev.*, 2012, **41**, 4113; (*c*) D. Lu, Md. D. Hossain, Z. Jia and M. J. Monteiro, *Macromolecules*, 2015, **48**, 1688; (*d*) F. Giacalone, V. Campisciano, C. Calabrese, V. L. Parola, Z. Syrgiannis, M. Prato and M. Gruttadauria, *ACS Nano*, 2016, **10**, 4627.

3 (*a*) S. Sadekar and H. Ghandehari, *Adv. Drug Delivery Rev.*, 2012, **64**, 571; (*b*) C. Deraedt, N. Pinaud and D. Astruc, *J. Am. Chem. Soc.*, 2014, **136**, 12092; (*c*) S. Svenson, *Chem. Soc. Rev.*, 2015, **44**, 4131; (*d*) Y.-H. Tang, M. Cangiotti, C.-L. Kao and M. F. Ottaviani, *J. Phys. Chem. B*, 2017, **121**, 10498.

4 (*a*) I. Taniguchi, S. Duan, T. Kai, S. Kazama and H. Jinnai, *J. Mater. Chem. A*, 2013, **1**, 14514; (*b*) X. Song, Y. Niu, Z. Qiu, Z. Zhang, Y. Zhou, J. Zhao and H. Chen, *Fuel*, 2017, **206**, 80; (*c*) K. J. Shah, T. Imae, M. Ujihara, S.-J. Huang, P.-H. Wu and S.-B. Liu, *Chem. Eng. J.*, 2017, **312**, 118; (*d*) S. J. Thompson, M. Soukri and M. Lail, *Energy Fuels*, 2018, **32**, 8658.

5 (*a*) C.-H. Lee, M.-R. Tsai, Y.-T. Chang, L.-L. Lai, K.-L. Lu and K.-L. Cheng, *Chem. – Eur. J.*, 2013, **19**, 10573; (*b*) E. Andreoli and A. R. Barron, *ChemSusChem*, 2015, **8**, 2635; (*c*) M. Mirzaie, A. Rashidi, H.-A. Tayebi and M. E. Yazdanshenas, *J. Chem. Eng. Data*, 2017, **62**, 1365; (*d*) C.-H. Lee, D. V. Soldatov, C.-H. Tzeng, L.-L. Lai and K.-L. Lu, *Sci. Rep.*, 2017, **7**, 3649.

6 (*a*) Y.-H. Jeong, M. Son, H. Yoon, P. Kim, D.-H. Lee, D. Kim and W.-D. Jang, *Angew. Chem., Int. Ed.*, 2014, **53**, 6925; (*b*) H. Lee, Y.-H. Jeong, J.-H. Kim, I. Kim, E. Lee and W.-D. Jang, *J. Am. Chem. Soc.*, 2015, **137**, 12394; (*c*) A. Krieger, J. P. F. Werner, G. Mariani and F. Gröhn, *Macromolecules*, 2017, **50**, 3464; (*d*) A. Arrigo, F. Puntoriero, G. L. Ganga, S. Campagna, M. Burian, S. Bernstorff and H. Amenitsch, *Chem*, 2017, **3**, 494.

7 (*a*) Y. Wang, Y. Lu, B. Gao, S. Wang, J. Ding, L. Wang, X. Jing and F. Wang, *Chem. Commun.*, 2016, **52**, 11508; (*b*) L. Zhao, S. Wang., J. Lü, J. Ding and L. Wang, *J. Mater. Chem. C*, 2017, **5**, 9753; (*c*) X. Ban, W. Jiang, K. Sun, B. Lin and Y. Sun, *ACS Appl. Mater. Interfaces*, 2017, **9**, 7339; (*d*) J. A. McEwan, A. J. Clulow, A. Nelson, R. D. Jansen-vanVuuren, P. L. Burn and I. R. Gentle, *ACS Appl. Mater. Interfaces*, 2018, **10**, 3848.

8 (*a*) B. Soberats, M. Yoshio, T. Ichikawa, X. Zeng, H. Ohno, G. Ungar and T. Kato, *J. Am. Chem. Soc.*, 2015, **137**, 13212; (*b*) R. Chico, E. de Domingo, C. Domínguez, B. Donnio, B. Heinrich, R. Termine, A. Golemme, S. Coco and P. Espinet, *Chem. Mater.*, 2017, **29**, 7587; (*c*) C.-X. Liu, H. Wang, J.-Q. Du, K.-Q. Zhao, P. Hu, B.-Q. Wang, H. Monobe, B. Heinrich and B. Donnio, *J. Mater. Chem. C*, 2018, **6**, 4471; (*d*) K. Albrecht, K. Matsuoka, K. Fujita and K. Yamamoto, *Mater. Chem. Front.*, 2018, **2**, 1097.

9 (*a*) I. Gracia, B. Feringán, J. L. Serrano, R. Termine, A. Golemme, A. Omenat and J. Barberá, *Chem. – Eur. J*, 2015, **21**, 1359; (*b*) S. Mula, S. Frein, V. Russo, G. Ulrich, R. Ziessel, J. Barbera and R. Deschenaux, *Chem. Mater.*, 2015, **27**, 2332; (*c*) B. Huitorel, Q. Benito, A. Fargues, A. Garcia, T. Gacoin, J.-P. Boilot, S. Perruchas and F. Camerel, *Chem. Mater.*, 2016, **28**, 8190; (*d*) M. Kumar and S. Kumar, *Polym. J.*, 2017, **49**, 85.

10 (*a*) I. M. Saez and J. W. Goodby, *J. Mater. Chem.*, 2005, **15**, 26; (*b*) H. Hahn, C. Keith, H. Lang, R. A. Reddy and C. Tschierske, *Adv. Mater.*, 2006, **18**, 2629; (*c*) M. Marcos, R. Martín-Rapúm, A. Omenta and J. L. Serrano, *Chem. Soc. Rev.*, 2007, **36**, 1889; (*d*) J. Vergara, N. Gimeno, M. Cano, J. Barberá, P. Romero, J. L. Serrano and M. B. Ros, *Chem. Mater.*, 2011, **23**, 4931; (*e*) K. Olofsson, O. C. J. Andrén and M. Malkoch, *J. Appl. Polym. Sci.*, 2014, **131**, 39876.

11 (*a*) I. M. Saez, J. W. Goodby and R. M. Richardson, *Chem. – Eur. J.*, 2001, **7**, 2758; (*b*) J. Barbera, R. Gimenez, M. Marcos and J. L. Serrano, *Liq. Cryst.*, 2002, **29**, 309; (*c*) J. M. Rueff, J. Barbera, B. Donnio, D. Guillon, M. Marcos and J. L. Serrano, *Macromolecules*, 2003, **36**, 8368.

12 (*a*) O. Haba, K.-I. Okuyama, H. Osawa and K. Yonetake, *Liq. Cryst.*, 2005, **32**, 633; (*b*) A. Belaissaoui, I. M. Saez, S. J. Cowling and J. W. Goodby, *Macromolecules*, 2013, **46**, 1268; (*c*) S. Hernández-Ainsa and J. J. Barbera, *Fluorine Chem.*, 2015, **177**, 37; (*d*) A. Concellón, M. Bucoș, J. L. Serrano, P. Romero and M. Marcos, *RSC Adv.*, 2016, **6**, 65179.

13 (*a*) J. Matraszek, E. Gorecka, J. Mieczkowski, M. Hejko and D. Pociecha, *Macromol. Chem. Phys.*, 2017, **218**, 1700316; (*b*) S. Herbst, B. Soberats, P. Leowanawat, M. Lehmann and F. Würthner, *Angew. Chem., Int. Ed.*, 2017, **56**, 2162; (*c*) P. Kumar, D. S. Shankar Rao, S. K. Prasad and N. Jayaraman, *J. Polym. Sci., Part A: Polym. Chem.*, 2017, **55**, 3665; (*d*) G. Zou, K. Luo, L. Zhao, H. Ni, H. Wang and Q. Li, *Liq. Cryst.*, 2018, **45**, 593; (*e*) C.-L. Wang, S. P. Prakoso and S.-L. Wu, *J. Chin. Chem. Soc.*, 2018, **65**, 368.

14 (*a*) K. Takagi, T. Hattori, H. Kunisada and Y. Yuki, *J. Polym. Sci., Part A: Polym. Chem.*, 2000, **38**, 4385; (*b*) A. E. Enciso, G. Doni, R. Nifosi, F. Palazzesi, R. Gonzalez, J. L. Coffer, E. E. Simanek, G. M. Pavan and A. A. Mohamed, *Nanoscale*, 2017, **9**, 3128; (*c*) S. Raut, A. E. Enciso, G. M. Pavan, C. Lee, A. Yepremyan, D. A. Tomalia, E. E. Simanek and Z. Gryczynski, *J. Phys. Chem. C*, 2017, **12**, 6946.

15 L. L. Lai, H. C. Hsu, S. J. Hsu and K. L. Cheng, *Synthesis*, 2010, 3576.

16 (*a*) L. L. Lai, C. H. Lee, L. Y. Wang, K. L. Cheng and H. F. Hsu, *J. Org. Chem.*, 2008, **73**, 485; (*b*) L. L. Lai, S. J. Hsu, H. C. Hsu, S. W. Wang, K. L. Cheng, C. J. Chen, T. H. Wang and H. F. Hsu, *Chem. – Eur. J.*, 2012, **18**, 8542; (*c*) L. L. Lai, S. W. Wang, K. L. Cheng, J. J. Lee, T. H. Wang and H. F. Hsu, *Chem. – Eur. J.*, 2012, **18**, 15361; (*d*) L. L. Lai, J. W. Hsieh, Y. H. Chang, M. Y. Kuo, K. L. Cheng, S. H. Liu, J. J. Lee and H. F. Hsu, *Chem. – Eur. J.*, 2015, **21**, 13336; (*e*) L. L. Lai, J. W. Hsieh, K. L. Cheng, S. H. Liu, J. J. Lee and H. F. Hsu, *Chem. – Eur. J.*, 2014, **20**, 5160; (*f*) M. R. Tsai, J. W. Hsieh, L. L. Lai, K. L. Cheng, S. H. Liu, J. J. Lee and H. F. Hsu, *J. Org. Chem.*, 2016, **81**, 5007.

17 (*a*) B. R. Kaafarani, *Chem. Mater.*, 2011, **23**, 378; (*b*) S. Kumar and H. K. Bisoyi, *Angew. Chem., Int. Ed.*, 2007, **46**, 1501.

18 B. Buchs (née Levrand), G. Godin, A. Trachsel, J.-Y. de Saint Laumer, J.-M. Lehn and A. Herrmann, *Eur. J. Org. Chem.*, 2011, 681.

19 R. Ziessel, G. Pickaert, F. Camerel, B. Donnio, D. Guillon, M. Cesario and T. Prange, *J. Am. Chem. Soc.*, 2004, **126**, 12403.

20 E. J. Foster, R. B. Jones, C. Lavigueur and V. E. Williams, *J. Am. Chem. Soc.*, 2006, **128**, 8569.